A Comparison of Special Helical Cutter Geometries Based on Cutting Forces for the Trimming of CFRP Laminates

Jean-François Chatelain and Imed Zaghbani

Abstract— Various tool materials exist that are capable of withstanding the abrasiveness and strength of Carbon fiber reinforced plastics (CFRPs), namely Diamond, Polycrystalline diamond (PCD) and coated carbide. While these materials offer high hardness, which is a key property for successfully machining CFRPs, only solid carbide offers the flexibility of different cutter geometries, accompanied by reasonable costs. This research analyzes the effects of two non-standard features added to cutters designed for CFRP machining. A standard helical geometry is compared to a cross-cut helical tool and a grooved flute tool based on cutting force analysis, surface roughness and delaminating. The cutters were used for detouring quasi-isotropic laminates with different thicknesses under various machining conditions. It was found that unstable cuts may occur during the machining of CFRP laminates. Some stable speeds and feeds were identified for the different cutters, and for these stable conditions, the force amplitude and profile were compared. It was found that adding features to the standard geometry significantly affects the cutting forces. While the cross cut geometry generates a compressive thrust force, the grooved geometry induces a quasi-null thrust force accompanied by less fluctuation of the feed force and the normal cutting force. It was also found that the cross cut tool damaged the laminates in terms of fibers pullout, voids and instability marks.

Keywords— Detouring, composites, CFRP, tool geometry, groove-teeth, cross cut, cutting forces.

I. INTRODUCTION

PRESENTLY, various tool materials exist that are capable of withstanding the abrasiveness and strength of Carbon fiber reinforced plastics (CFRPs), namely Diamond, Polycrystalline diamond (PCD) and coated carbide. While these three materials offer high hardness, which is a key property for

J-F. Chatelain is professor with the Department of Mechanical Engineering at École de Technologie Supérieure, Université du Québec, Montréal, Québec, Canada, H3C 1K3 (phone: 514-396-8512; fax: 514-396-8530; e-mail: jfchatelain@mec.etsmtl.ca)

Imed Zaghbani is research associate with the Department of Mechanical Engineering at École de Technologie Supérieure, Université du Québec, Montréal, Québec, Canada, H3C 1K3 (e-mail: imed.zaghbani@etsmtl.ca).

successfully machining CFRPs, only solid carbide offers the flexibility of different cutter geometries, accompanied by reasonable costs. The efficiency of a carbide cutter is determined by the coating and the cutting edge geometry. The cutter geometry can be defined by different angles in the tool-in-hand system, the tool-in-machine system or the tool-in-use system [1]. For an end mill cutter, the principal angles that significantly affect the cutter performance are the rake angle, the clearance angle, the tool nose radius and the helix angle.

The cutting tool's rake angle is the angle between the cutting edge and the cut itself, and it may be positive, negative, or neutral. The first allows lower cutting forces, while the latter provides a stronger tool wedge. For CFRP machining, both geometries have major impacts on the chip formation mode [2]. For unidirectional laminates, the chip formation mode is primarily a combination of the fiber orientation angle and the cutter rake angle [3]. The rake angle may also affect the quality of the machined surface, and increasing the rake angle improves the overall quality of the machined edge [3]. The clearance angle prevents the cutter from rubbing against the machined surface. For composite materials, this is the angle that controls the bouncing of fibers on the clearance face, and as a result, the clearance angle may therefore affect the cutting forces [2]. Furthermore, it was observed that using large clearance angles improves the edge quality of the machined laminates [4]. Another important tool geometry parameter is the nose radius. The tool nose radius is the angle formed by the point of the tool; it may be large, for high strength operations needed when roughing parts, or sharp, for fine operations needed during finishing operations. Generally, the cutter edge is prepared with particular shapes in order to strengthen it. Those shapes include a honed radii, a chamfer, a nose radius and, or a combination of all three. For composite materials, cutters with honed radii are preferred, especially when they are sharp. A cutter is deemed to be sharp enough when its nose radius is less than the fiber diameter. Generally, the fiber diameter ranges between 5 and 20 μm. However, a very low nose radius can weaken the cutter, making plasticization of the edge cutter possible under the resistance of the strong fibers. It has been experimentally proven that for CFRP, the nose radius affects the chip formation mode [5].

Finally, it is important to address the influence of the helix angle, which is the angle formed by a line tangent to the helix and a plane through the axis of the cutter. Generally, for metallic alloys, end mills with small helix angles develop the

greatest cutting force and surface roughness [6]. In fact, if the flutes were straight, the whole tooth would impact the material at once, causing the cutter to have the same axial chip load along its axis. This is the main reason why the effect of the helix angle is negligible when the laminate thickness is small. In fact, if the depth of cut is less than 5% of the helix pitch, the effect of the helix angle will be negligible due to the low variation of the axial chip load along the cutter axis [7]. This means that for a thin laminate, the use of a straight or helical angle will have a similar effect. Generally, helical cutters generate a higher axial force than do straight cutters. Acting normally on the laminate, this axial force causes delamination and fuzzing in the surface ply, which is not supported in the force direction [8,9]. To reduce the effect of the unidirectional axial force, new cutters utilizing a double helix are proposed by manufacturers. The two helixes are opposed, which may generate compression from both sides of the laminate, and thus prevent delamination. Another compromise to this geometry is a grooved tooth. Instead of creating a macro helix angle on the whole body of the cutter, it is possible to create a smaller helix angle on each tooth. If repeated along the tooth, the grooves will present a sort of micro helix angle. Such a geometry would be expected to reduce the cutting forces and enhance the cutter performance. An example of a grooved tooth end mill is presented in Figure 1.

Various studies in the CFRP machining field have been interested in the standard definition of the tool geometry (helix angle, rake angle, clearance angle and nose radius). Other works relate on the modelling of the cutting process or to the effect of the machining parameters on the surface finish [10, 11]. However, to the authors' knowledge, the matter of special features has not been covered in depth. The goal of the present study is to evaluate the effects of two non-standard features added to cutters designed for CFRP machining. The comparison will be based on cutting force analysis, surface roughness and delamination. To that end, this paper is organized as follows: the first section deals with the methodology adopted for the experimental work, followed by a discussion of the results, focusing on the analysis of the effects of special features on both force amplitude and profile. These are followed by an analysis of the resulting surface finish and the part delamination.

II. METHODOLOGY

The laminates for machining tests were prepared in a controlled aeronautical environment using pre-impregnated technology. The stack having 64% of fiber volume fraction was autoclave-cured. The orientation of the plies was such that the quasi- isotropic properties of the laminates were obtained. The layer orientation and laminate thickness are summarized in Table 1.

Fig. 1: Example of grooved tooth geometry

Table 1: Properties and configuration of the machined CFRP laminates

	Thickness [mm]	Volume fraction	Total number of plies	Average ply thickness [mm]	Ply orientation
P1	3.47	64%	24	0.144	4/8/8/4
P2	4.63	64%	32	0.144	6/10/10/6
P3	5.79	64%	40	0.144	8/12/12/8

The presence of major processing defaults can represent the first source of cutting force signal distortions, and if major defaults are present, it becomes difficult to interpret or model the cutting forces. The square-shaped laminates were therefore inspected prior to machining. A C-Scan was used to verify the absence of any major processing defaults. Once inspected, the laminates were pre-drilled for tightening on a machining fixture, as shown in Figure 2, where the experimental set-up is presented. The pre-drilling was necessary both for screwing the laminate to the fixture and in order to facilitate the smooth entry of the cutter in the laminate when detouring each coupon using different cutting conditions.

The Figure 3 shows the aluminum back plating system (#2) using 49 screws and a torque wrench to secure the laminate (#1). Detail A shows a sample of a machined test coupon. Each side of the squared sample was machined under specific cutting conditions, and different combinations of cutting parameters were tested. The subassembly (laminate and back plate) was tightened to a three-axis dynamometer table type Kistler 9255B (#3).

The charge amplifiers generate five output signals transmitted to a data acquisition card (type DT-9836). The sampling frequency was set at 48 kHz/canal, for a recording time of 16 seconds. A USB communication protocol was used to interpret the output signals of the data acquisition card, with a Matlab-based signal processing program.

The measurement system was statically and dynamically calibrated on an MTS tension machine. Both static and dynamic calibration allowed the estimation of the drift errors and their correction if they exceeded the acceptable limit of ± 10 mN/s for the three directions. To allow the detection of the slightest chatter signals, no filter was applied on the force signals. The signals were exported to Matlab for further analysis. All machining tests were realized under dry conditions using the same tool geometry. The configuration of the proposed setup enables to test 168 different machining conditions. The plan of experiments performed is presented in table 2. Six cutting speeds and six feedrates were tested for each cutting tool. The plan considers the cutting mode, e.g up milling and down milling since the slot trimming produces each mode on two different square samples on opposed sides. The analysis performed on the resulting force signals for some

of these cutting parameters and for different tool geometries is presented in the following sections.
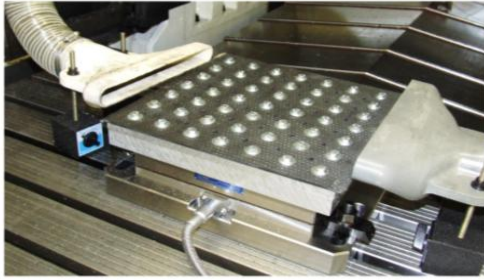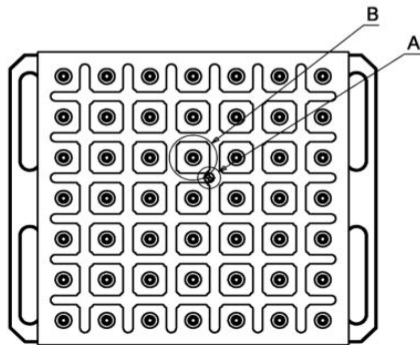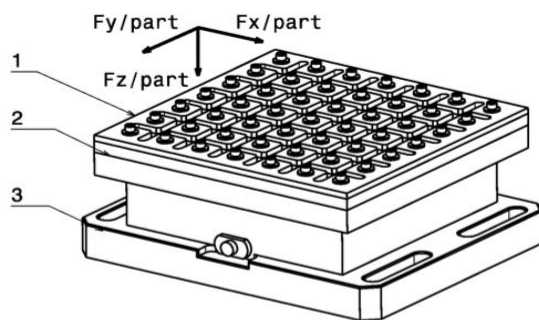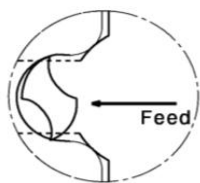

Fig. 2: Experimental set-up for dry trimming of CFRP with different cutting parameters
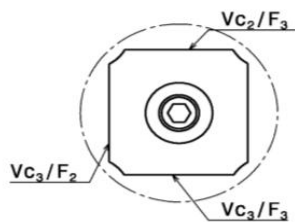

Fig. 3: Experimental set-up (details A and B)

Table 2 Plan of experiments

Cutting speed (m/min)	Feed (in/rev) / (mm/rev)	Thickness
200 (6 683 rpm)	0.004 / 0.10	24 plies 3.47 mm
300 (10 025 rpm)	0.008 / 0.20	
400 (13 367 rpm)	0.010 / 0.25	32 plies 4.63 mm
500 (16 709 rpm)	0.014 / 0.37	
650 (21 721 rpm)	0.016 / 0.4	40 plies 5.79 mm
800 (26 734 rpm)	0.020 / 0.5	

III   RESULTS AND DISCUSSION
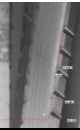
A. Tool Geometry and Stability

As earlier mentioned, different tool geometries were used to machine the CFRP laminates, and their descriptions are summarized in Table 3. The last column of the table shows the cutting tools pictures recorded with a 5X magnification factor.

From the results presented in Figure 4, it can be observed that tools C1 and C3 provide similar results in terms of cutting force profiles. The two cutters have similar geometries, which explain the same profile obtained for the X cutting force component in terms of amplitude and shape. A similar result is observed for the Y component. The recorded force signals when machining with the C6 cutter are much higher than with the other two cutters. In fact, the axial cutting force is 5 to 10 times higher than regular geometries. The high amplitudes observed in the three cutting directions for tool #C6 are most probably due to a dynamic instability. To confirm the presence of such instability, a Fourier analysis of the recorded signal in the steady-state period was conducted, which is a common approach [12]. The results obtained are plotted in Figure 5.

The spectra of the F_x, F_y and F_z forces show that the totality of the signal energy is carried by a single 3809 Hz frequency. The latter is neither a harmonic of the spindle speed (111.4 Hz) nor a harmonic of the tooth passing frequency (668.4 Hz). The dynamic instability was also confirmed by sound recording during the cutting test. The presence of a sharp sound was noticed during machining. In the author's opinion, the instability was due to a combination of two causes:

1. The laminate width is thinner than the cross cut part of the cutter.
2. The selection of a spindle speed close to a resonance of the system tool-part-machine.

Table 3 Description of tool geometries

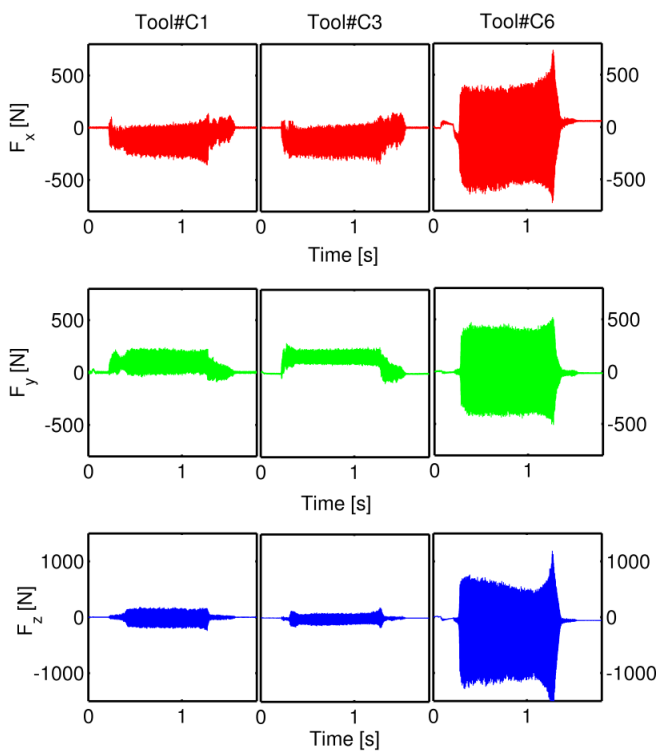| Tool#	Flute number	Dia. (mm)	Material	Helix angle	Rake angle	flank angle	
#C1	8	10.00	Carbide CVD coating	10°	10°	15°	
#C3	8	9.525	Carbide CVD coating	10°	10°	15°	
#C6	6	9.525	Carbide CVD coating	±30°	20°	15°	

Fig. 4 Effect of tool geometry on cutting force profile for low speed and low feed (200 m/min and 0.1 mm/rev)

If one of the above factors is altered, the instability will disappear. The spindle speed was increased from 111.4 Hz to 166.6 Hz. Figure 6 summarizes the recorded cutting forces in the X, Y and Z directions and their corresponding spectra, using a fast Fourier transformation.
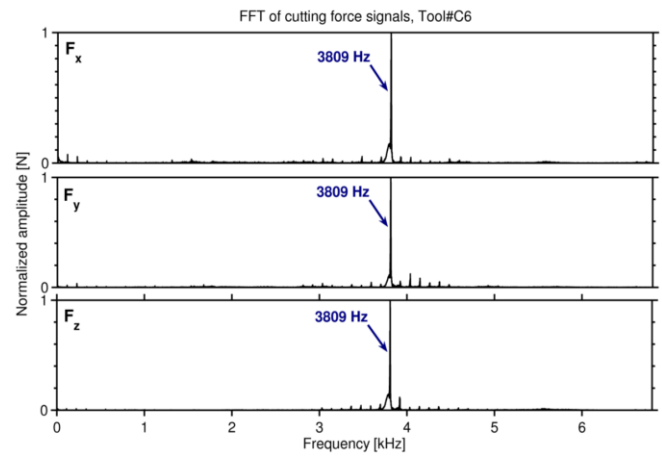

Fig. 5 FFT analysis of the cutting forces in the three machining directions @200 m/min and 0.1 mm/rev

It can be observed that the amplitude of the cutting forces was significantly reduced. The FFT analysis demonstrated the absence of instability, and the signal energy carried was distributed on the spindle frequency and its harmonics. The absence of an amplified non-harmonic frequency attests to the nonappearance of dynamic instability. However, dynamic instability was repeatedly observed for several combinations of feed and speed, meaning that the cross cut geometry needs to select cutting parameters with care. In the author's opinion, for the case of CFRPs, this geometry is less adequate for laminates having a thickness smaller than the cross part of the cutter. The previous analysis revealed the need for dynamic stability, which should enable a comparison of the geometry effect. One of the major challenges encountered was retrieving a feed and speed that are dynamically stable for the four tested geometries. A stable cut is characterized by a "clean" spectrum, where only the harmonics of the spindle speed can be observed. If the recorded force signal is plotted in the time domain, a stable profile of a cutting force signal will appear.

A. Effect of Tool Geometry on the Profile

Adding special features to the standard tool geometry affects both the general and the per revolution profile. A comparative graph is plotted in Figure 7, showing the cutting forces in the x direction for the three different geometries. The first period (Zone I) corresponds to the engagement of the tool in the part. This zone is characterized by a partial engagement of the cutter in the part. The cutter engages in the workpiece, bringing a high amount of energy to the machined part. The force profiles of zones I and III, which are the transient periods, look very similar for the C1 and C3 geometries (Figs. 7a and 7c). For the third geometry C6 (Fig 7e), the tool entry and exit are much smoother.

During the next period, the cutter advances smoothly in the part. Once the cutter is fully engaged, the cutting forces reach the second zone (Zone II), the steady state period, which is characterized by a repetitive cutting force profile from one revolution to another. It is also characterized by nearly constant force maximum amplitude for each period. Regarding
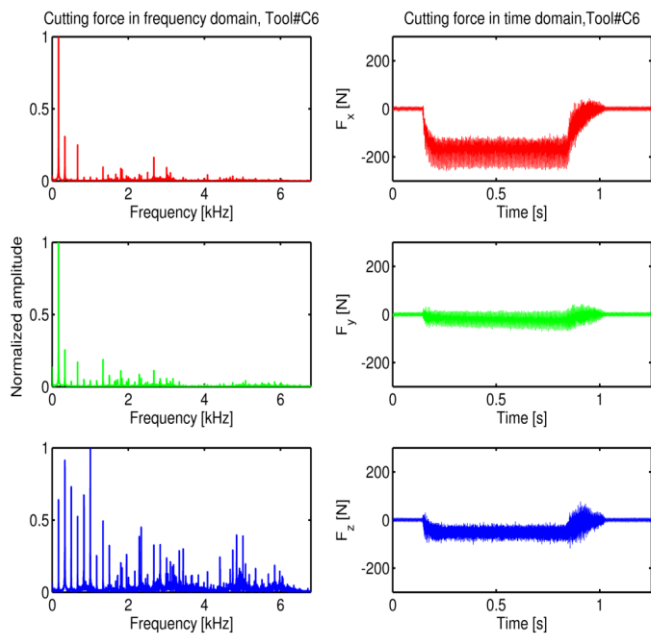
Fig. 6 Cutting forces in frequency and time domain showing process stability when the cross cutter (#C6) was used @300 m/min and 0.2 mm/rev

the force per revolution, the three geometries presented four different lots, with each lot corresponding to one tool revolution.

It can be seen that the highest fluctuation is observed for the standard cutter. The force fluctuation can be evaluated by the peak-to-peak value corresponding to the maximum force minus the minimum force. Figure 7 (b, d and f) presents the cutting force in the X direction during 4 revolutions of the cutter. The force profile for each passing tooth of the cutting tool can be clearly identified in the figure. Each peak of the force profile presents the passage of a tooth. The cutting force starts with a quasi-null value when the tool is engaged, and then the cutting force increases until it reaches a maximum at full tooth engagement with respect to X axis, and then decreases until the tooth separates from the workpiece, giving way to the second tooth. The next tooth follows a similar profile as the first tooth. The engagement of more than one tooth is obvious in the figure, as the instantaneous cutting force continuously increases in one revolution. The addition of grooves smoothes the force profile making the fluctuation less sudden (C1 compared to C3). It can be concluded that the smoothing of the force profile is significant when using grooved cutter.
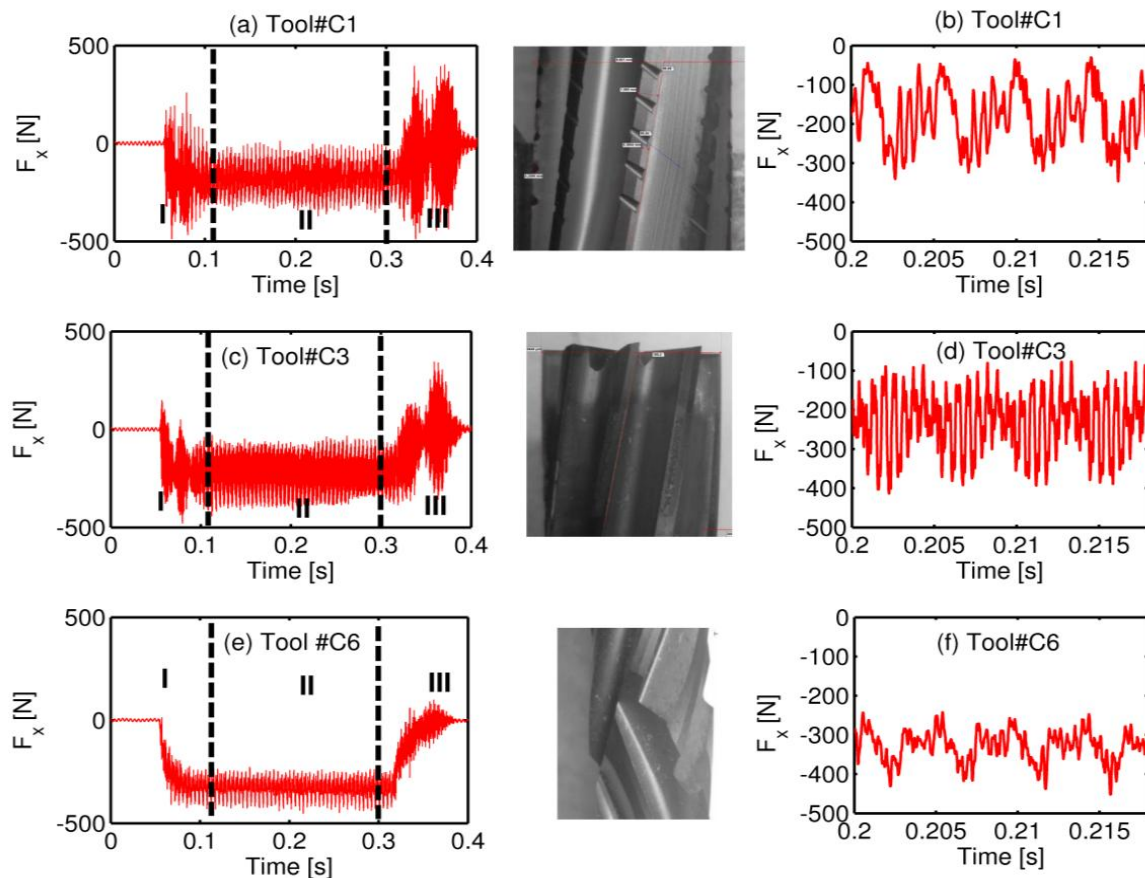

Fig.7 Cutting forces over 4 revolutions for stable conditions @400 m/min and 0.4 mm/rev when detouring a 24-ply laminate

B. *Effect of Tool Geometry on Force Magnitude*

The forces exerted on the laminate during milling are characterized by a profile and amplitude, and any damage observed on the final part is a combination of these two characteristics. Figure 8 presents the amplitude of the cutting forces for each tool's geometry for the steady state period (zone II)**.** The fluctuation in amplitude observed is due essentially to the sinusoidal variation of the chip thickness.

The highest amplitude cutting forces were recorded in the feed direction X for the three geometries. This amplitude can be characterized by different mathematical descriptors, and the peak-to-peak value can properly describe the observed fluctuation. The highest peak-to-peak value is recorded for the standard geometry in the X direction, most probably due to the reduction of the high contact surface of cutter teeth in the cutting zone. This led to a higher rate of material removal at each tooth, which significantly increased the recorded amplitude of the feed cutting force. When, for the Y direction, the highest amplitudes are recorded for the grooved geometry which implies an increase of the abrasion between the cutter and the machined part surface.

However, the grooves contribute to significantly decrease the axial forces Fz. On the other hand, the standard geometry enhances the fluctuation of this force component between two maxima: one negative, and the second, positive. This fluctuation may cause significant damage to the laminate. The cross geometry contributes to eliminate this fluctuation by generating a directive cutting force, which is negative, meaning that force exerted on the laminate is compressive. Despite this result, the authors observed that the worst damage cases were caused by the cross cut geometry, which is discussed in the following section. To appreciate the difference regarding the axial force component of all three

cutting tools, Figure 9 is a plot showing the evolution of this force with respect to the feedrate for specific conditions of the plan of experiment, e.g. a 24 ply laminate and a cutting speed of 650 m/min. The difference between cutters C1 and C3 is as high and almost equivalent to the difference between cutters C3 and C6. Also, this difference increases with the feedrate and the same relationship is found for other speeds and laminate thicknesses, having stable cuts.

C. *Quality of Laminates*

The quality of the laminates after trimming was compared in terms of surface defects and material integrity through visual, microscopic and C-scan inspection. The effect of tool geometry on the surface quality is presented in Figure 10 and Figure 11. The presented samples in the figures were machined under the same cutting parameters using the three different geometries. The visual inspection shows that most of the specimens trimmed using the cross cut tool C6 were severely damaged, with uncut and peeled-up fibers. An example is presented in Figure 10. This may be due to the higher axial forces measured for this cutter but also to the dynamic component of the acting forces.

In fact, it can be observed that the general topography of the generated surfaces issued from the trimming process is different for each different tool (Fig. 11). The most remarkable effect of tool geometry is the presence of instability marks in the case of the cross cut geometry. Examples of these marks are indicated using arrows in Fig.c. The other specimens that were cut using the grooved and the standard cutters did not show any of these damages, neither uncut fibers nor instability marks, for all conditions of the plan of experiment.
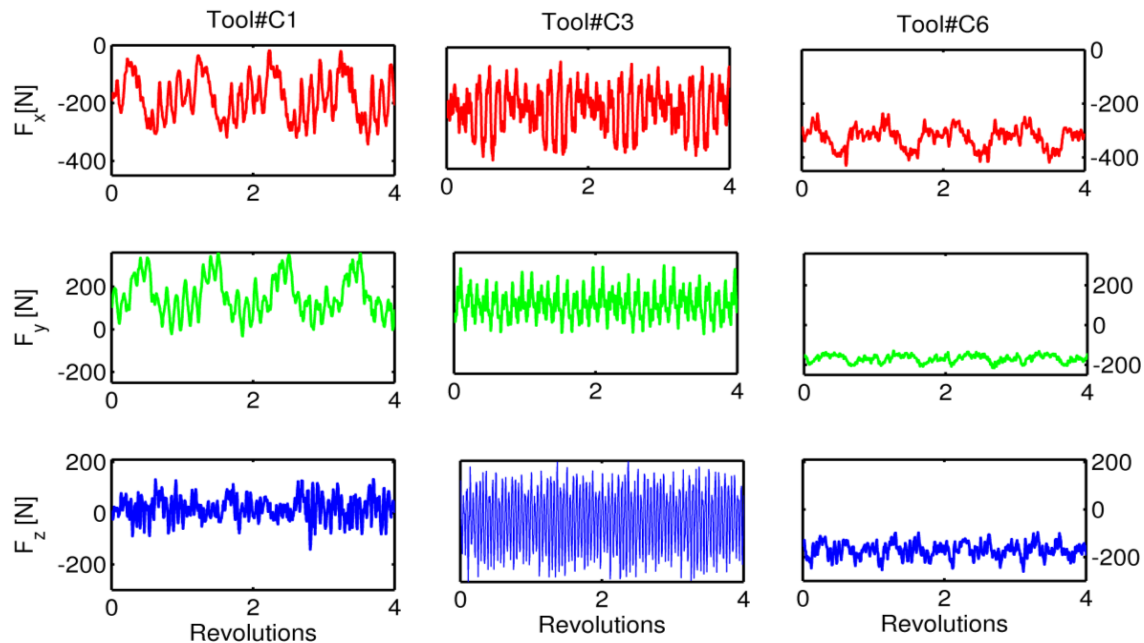

Fig. 8 Cutting forces over 4 revolutions for stable conditions @400 m/min and 0.4 mm/rev when detouring a 24-ply laminate
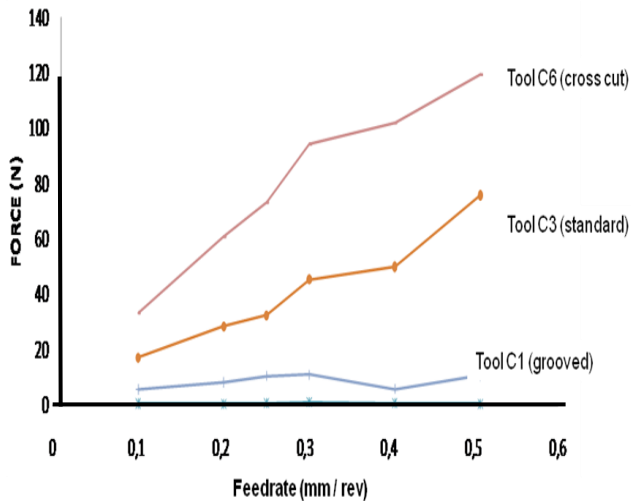
Fig. 9 Axial force component as a function of feedrate (Vc=650 m/min, 24 ply laminate)

Fig. 10 Example of uncut fibers produced from the cross cut cutting tools

A common characteristic between the three geometries is that the worst quality is observed at the plies oriented at 135 degrees. This is most probably not due to the tool geometry nor the cutting conditions. The main reason could be the cutting mode. In fact when the fibres are oriented at 135 deg, they are extensively bent before being broken. This leads to observable voids on the machined surface as presented in figure d, e and f. These voids are less frequent in the case of cutter C1. This effect was most probably induced by the grooves that have reduced the level of cutting forces. Nevertheless they become more recurrent tin the case of cutters C3 and C6.

The effect of the cutter geometry on the level of reached temperature can be observed in the 0 degree orientation. Apparently, the temperature level reached when using the cutter C6 is the highest. It can be observed that the resin matrix is thermally damaged and spread all over the ply at 0 degree orientation. This may be due to higher friction caused by this cutter conjugated with low dynamic instability. Both factors lead to increasing the temperature to be above the transition temperature of the resin, as studied also by Iliescu [13].
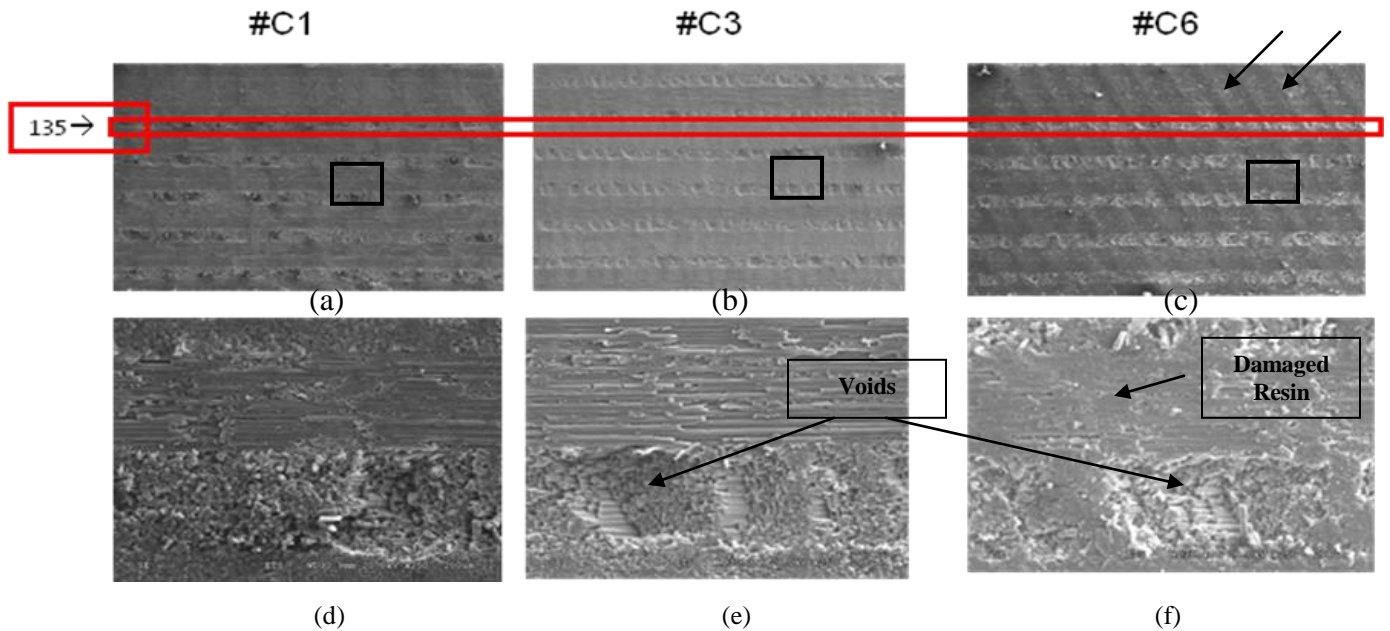

Fig. 11 Micrographs of trimmed CFRP using the grooved (C1), the standard (C3) and the cross cut (C6) cutting tools (250X)

IV CONCLUSION

The cutting forces provide a good indication of cutter performance. These forces give clear insights about the cutter during different phases of machining. However, to be useful, the forces must be recorded under stable conditions. In this study, different combinations of cutting conditions were conducted in order to find commonly stable conditions for three cutters with different geometries. These geometries were developed especially for the detouring of CFRP laminates. It was found that the cross cut geometry is more sensitive to instability than standard and grooved geometries. However, this cross cut geometry generates a compressive thrust force, which is the opposite of the standard geometry. It was found that the special grooves reduce the axial force to approximately a null value; in addition, they significantly reduce the fluctuation of the feed and normal cutting forces.

REFERENCES

[1] Astakhov, V.P., Geometry of Single-Point Turning Tools and Drills: Fundamentals and Practical Applications (Springer, 2010).

[2] Sheikh-Ahmad J-Y., Machining of Polymer Composites, Springer Science, 2009.

[3] Kaneeda, T., CFRP cutting mechanism. Transaction of North American Manufacturing Research Institute of SME 19, 216-221, 1991.

[4] Arola, D., Ramulu, M., Wang, D.H., Chip formation in orthogonal trimming of graphite/epoxy, composite. Composites: Part A 27A, 121-133, 1996.

[5] Wang, X.M., Zhang, L.C., An experimental investigation into the orthogonal cutting of unidirectional fiber reinforced plastics. International Journal of Machine Tools and Manufacture 43, 1015-1022, 2003.

[6] S. and R. Davies, Cutting performance of end mills with different helix angles, International Journal of Machine Tools and Manufacture, Volume 29, Issue 2, pp. 217-227, 1989.

[7] Tlusty J., Upper Saddle River, N.J.: Prentice-Hall, 2000.

[8] Wang, D.H., Ramulu, M., Arola, D., Orthogonal cutting mechanisms of graphite/epoxy composite. Part I: Unidirectional laminate. International Journal of Machine Tools and Manufacture 35, 1623-1638, 1995

[9] Bhatnagar ,N., Ramakrishnan, N., Naik, N.K., Komanduri, R., on the machining of fiber reinforced plastic (FRP) composite laminates. International Journal of Machine Tools and Manufacture 35, 701-716, 1995.

[10] Schlegel, D., Folea, M., Roman, A., Nardin, P., Surface Analysis of Machined Fiber Glass Composite Material, Recent Researches in Manufacturing Engineering, WSEAS MEQAPS, Brasova, pp 152-155, 2011.

[11] Iliescu,M., Spanu, P., Rosu, M., Comanescu,B., Simulation of Cylindrical-Face Milling and Modeling of Resulting Surface Roughness when Machining Polymerci Composites, Proc. Of the 11th WSEAS Int. Conf. On Automatic Control, Modeling and Simulation, ACMOS, Istanbul, pp. 219-224, 2009.

[12] Frumusanu, G., Epureanu,A., Constantin,I., Cutting process stability Evaluation by process parameters monitoring, Proc. Of the 8th WSEAS Int. Conf on Non-linear Analysis, Non-linear Systems and Chaos, Lalaguna, p. 345-350, 2009.

[13] Iliescu, M., Spanu, P., Bardac, D., Research on Temperature Distribution Field in Milling Glass Fibers Reinforced Polymeric Matrix Composites, Proc. Of the 10th WSEAS Int. Conf on Mathematical and Computational Methods in Science and Engineering (MACMESE 08), Bucharest, pp. 380-383, 2008.